Weak magnetic field effects in biology are measurable—accelerated *Xenopus* embryogenesis in the absence of the geomagnetic field

Alessandro Lodesani,[1,*] Geoff Anders,[1,2,†] Lykourgos Bougas,[3] Tobias Lins,[4] Dmitry Budker,[3,5,6,7] Peter Fierlinger,[4] and Clarice D. Aiello[1,‡]

[1]*Quantum Biology Institute, Los Angeles, USA*

[2]*Leverage, USA*

[3]*Johannes Gutenberg-Universität Mainz, Mainz, Germany*

[4]*Technische Universität München, Munich, Germany*

[5]*Helmholtz Institute Mainz, Mainz, Germany*

[6]*GSI Helmholtzzentrum für Schwerionenforschung GmbH, Darmstadt, Germany*

[7]*Department of Physics, University of California, Berkeley, USA*

(Dated: October 10, 2024)

Despite decades of reports of weak magnetic field effects in biology across the tree of life and on a broad range of cell types, the evidence to date remains met with skepticism. To remedy this, we present open-data, large-scale, and varied morphological evidence that *Xenopus laevis* embryo development is accelerated in a well-engineered, environmentally-calibrated hypomagnetic field of less than 1 nT. These data imply that basal tadpole physiology can sense and react to the absence of Earth's minute magnetic field of approximately 50 μT. The effect is significant, as demonstrated by a variety of statistical measures. As no definitive biophysical mechanism has been identified to account for its occurrence, this study raises the question of which mechanism provides the most plausible explanation. How that question is answered may have implications in a variety of fields, including human health, behavioral ecology, and space exploration.

The main text and supplementary information are available for download as a single, cross-referenced .pdf file with clickable links at bit.ly/Weak-magnetic-field-effects-in-biology-are-measurable.

* alessandro@quantumbiology.org

† geoff@quantumbiology.org

‡ clarice@quantumbiology.org

1. Summary

The biological effects of weak magnetic fields, such as Earth's geomagnetic field ($\sim 50\ \mu$T), have long been reported, but remain poorly understood and met with skepticism [1, 2]. This scientific stalemate is due both to the absence of a definitive biophysical mechanism to explain such effects, and to experimental shortcomings. First, the rationale has been that the biological effects of weak magnetic fields are negligible because the field strengths are thought to be too small to trigger a biophysical sensing mechanism. Second, large-scale, thoroughly environmentally controlled data are lacking, and existing results are often ambiguous regarding whether the effects are truly attributable to magnetic fields or other environmental factors. However, the reality of a given effect can be established absent a known mechanism with a sufficiently well-designed experiment. Here, we demonstrate that the development of *Xenopus laevis* embryos is significantly accelerated when they are raised in a hypomagnetic environment (< 1 nT) shielded from Earth's geomagnetic field. Our large-scale dataset and analysis code are publicly available. After extensive calibration of environmental conditions, our assessment is that the origin of the effects is the absence of Earth's magnetic field. Our main finding is thus that the basal physiology of a non-migratory species like *Xenopus laevis* significantly reacts to a magnetic shift on the order of 50 μT, with effects observed as early as one day post-fertilization. These results are sufficiently robust to advance the scientific consensus that weak magnetic fields indeed exert measurable biological effects. We also raise the question of which underlying mechanism could best explain our observations. Answering this could have far-reaching implications across fields such as human health, behavioral ecology, and space exploration.

2. Introduction

Weak magnetic field effects in biology have been reported for many years [1]. Reported effects are wide-ranging, from the up- and down-regulation of cell proliferation [2], to DNA repair [3], to cellular respiration and metabolism [4, 5], to cytoskeleton configuration [6, 7], and ion channel functioning [8]. There are also established migratory phenomena, such as the ability of birds to navigate at dusk, which are presumed to depend on Earth's magnetic field [9], which is itself very weak.

Nevertheless, these magnetic effects have remained controversial. First, weak magnetic fields (we consider shifts of ~ 1 mT, on the order of a cell phone's field [10], or smaller to be 'weak' for the purposes of this paper) are broadly not expected to be strong enough to have any noticeable effect on biological organisms. Second, the magnitude of reported effects does not vary directly with field intensity, yielding uncertainty about the underlying mechanism. The reality of a given effect can be established absent a known mechanism with a sufficiently well-designed experiment. However, until now the studies of weak magnetic field effects in biology have suffered from shortcomings, ranging from small sample sizes to inadequately controlled conditions.

In our experiment, we raise *Xenopus laevis* frog embryos in a carefully constructed hypomagnetic chamber. The chamber, in combination with compensation coils, subtracts the Earth's magnetic field (of approximately 50 μT), yielding a hypomagnetic condition of less than 1 nT, close to zero. We examine over 2,750 tadpoles over 10 batches. The first seven batches have *Xenopus* embryos, raised in individual wells, divided randomly between the hypomagnetic condition and a control condition, which is a deactivated cell incubator with comparable light, humidity, and temperature conditions. Of these, the first three batches were used to identify a plausible hypothesis, namely, that *Xenopus* embryos raised in a hypomagnetic condition experience accelerated development; the remaining four batches test this hypothesis. We then raise three further batches of embryos in a positive control, where the Earth's magnetic field is recreated inside the hypomagnetic chamber, and embryos are again divided between the hypomagnetic chamber and the deactivated incubator.

Using a variety of objective morphological measures, we find significant differences between the tadpoles raised in the hypomagnetic condition and the regular and positive controls. Differences, which pertain to both the shape and color of the embryos, are visible upon inspection and are confirmed by a variety of statistical tests, where the role of human judgment is reduced as much as possible. The differences appear on day 1 post-fertilization and are present on days 2 and 3 post-fertilization; on day 3, the embryos are preserved in formalin. The differences we observe are consistent with those observed by other labs, both those that studied the effects of minutely increasing and decreasing the intensity of magnetic fields experienced by *Xenopus* embryos. All of our data has been made publicly available.

This experiment solidifies direct observational evidence for weak magnetic field effects in a particular biological system. Since we remove a pre-existing magnetic field, rather than applying a new one, it follows that *Xenopus* development is impacted by Earth's magnetic field. *Xenopus* is not migratory, so there is no reason to expect that it would evolve mechanisms to navigate using Earth's magnetic field, especially as early as day 1 post-fertilization. There are also no indications of magnetite, as in magnetotactic bacteria, or conduction channels, like those in sharks and rays. This raises the question of the mechanism and biological significance of the effect, which we speculate on only briefly.

Historically, our experiment bears some resemblance to that of Francis Hauksbee [11], who in the early eighteenth century used a sophisticated air pump to create a superior vacuum condition for studying electricity. In this case, rather than an air pump, we use a mu-metal and copper-shielded box; rather than bringing air pressure close to zero, we bring the magnetic field close to zero; and rather than confirming the electrical nature of light emitted by frictional processes, we confirm that weak magnetic field effects in biology are measurable.

3. The experiment is well-controlled, with magnetic field environment as the only significant variable

We chose *Xenopus laevis* for our experiments because it is a widely used model organism in embryology, with straightforward husbandry and embryos that can be raised at room temperature (Supplementary Section SI1). Frogs are mostly non-migratory, with known exceptions of magnetic geofield sensing during pond changes [12]; we see no clear evolutionary advantage for *Xenopus laevis* in being able to sense Earth's weak magnetic field early in embryogenesis. Our selection of *Xenopus* is thus based on how common it is, rather than on any desired organismal trait.

For three days, we raise each tadpole individually in the wells of 24- or 48-well plates, with a total of over 2,750 tadpoles. This setup disrupts chemical communication between tadpoles, completely prevents cross-contamination, and, most importantly, allows us to monitor the morphological development of each individual. All plates are prepared at the same time and filled with 0.1x Marc's Modified Ringer's (MMR) solution (Supplementary Section SI2) from the same bottle. After *in vitro* fertilization (Supplementary Section SI2) and egg randomization (Supplementary Section SI3), embryos are placed in either a hypomagnetic or control environment (*i.e.*, exposed to Earth's ambient magnetic field) and left undisturbed for 24 hours, with the plates' plastic lids on. Imaging is performed approximately every 24 hours post-fertilization (p.f.) for three days (Supplementary Section SI4). Day 1 and 2 imaging sessions are usually completed in well under an hour, since the embryos are not motile, while day 3 tadpoles are fixed in formalin prior to imaging. Typical images for each day are displayed in panel **c**) of Fig. 1; the entirety of our image database, along with all developed code, is organized and accessible in the project's GitHub depository (a guide is found in Supplementary Section SI69). We perform one *in vitro* fertilization per week, with the resulting tadpole populations referred to as 'batches' (*e.g.*, batch B2 is the second batch; for a batch overview, see Supplementary Section SI5).

The hypomagnetic chamber, depicted in panel **a**) of Fig. 1, is a multi-layered metal enclosure designed to block ambient magnetic fields primarily through passive shielding. Its residual magnetic field is measured at less than 1 nT. Details on the chamber and the magnetic

calibration procedure are provided in Supplementary Section SI9. Between batches B5 and B6, the chamber, which initially shielded only against DC and low-frequency fields using mu-metal, was upgraded with a permanent copper shell to block AC fields as well. Calibration curves thus refer to either the initial configuration ('DC shielding') or the final configuration ('AC+DC shielding'). Tadpole rates of embryogenesis inside the chamber before and after copper shielding installation are similar, adding strength to the proposition that the observed biological effects are due to DC field shielding. Tadpoles in the control group are kept inside a closed, but switched off, cell incubator. This environment is referred to as the 'control box' (see Supplementary Section SI10); Earth's weak DC magnetic field permeates the control box. Batches B1–B7 are regular experimental runs; batches denoted +1–3 are positive control runs, where a magnetic field mimicking Earth's is artificially applied inside the hypomagnetic chamber (see Supplementary Section SI11).

Environmental factors that are known to perturb embryogenesis were recorded for the two environments. Sensors were excluded from the experimental environments during runs to prevent interference with the ambient magnetic field, so all calibrations were conducted separately under carefully replicated conditions. A thorough discussion about the effects of environmental factors, including a comparison of humidity, pressure, and light intensity and spectrum is provided in Supplementary Section SI12. Light levels are low, with 0.0873 ± 0.0003 lux in the control box and 0.0751 ± 0.0002 lux in the hypomagnetic chamber. Curves of temperature are presented in panel **b**) of Fig. 1.

Temperature is a critical factor regulating the speed of *Xenopus* embryogenesis: Warmer temperatures accelerate development [13]. Before installation of the AC shielding (batches B1–5), the temperature was up to half a degree lower in the hypomagnetic chamber than in the control box. After the AC shielding was added (batches B6–7), this temperature difference shifted slightly, with the hypomagnetic chamber now being marginally warmer by 0.10–0.15°C. In positive control runs (batches +1–3), the heat generated by the coils further increased the temperature difference to approximately 0.45°C. All those figures are conservative; actual temperature differences are likely less pronounced due to thermalization with the lab environment (details in Supplementary Section SI12).

After thoroughly assessing temperature, light levels, humidity, and pressure between the hypomagnetic chamber and the control box, we conclude that any observed significant effects are most likely due to the difference in magnetic field conditions between them.

In our experiments, we detect significant variability in the developmental speed of embryos across different weekly batches. This variability does not appear to arise solely from the use of different females as the egg source every week (see Supplementary Section SI6). Although not extensively documented in the literature—with the exception of one comprehensive study [14], which reaches a similar conclusion—we suspect that such variability is a common occurrence that remains largely unreported; we have reported and quantified it in a way that we believe is adequate and meets or exceeds the standards of the field.

Despite the large batch-to-batch variability, we can qualitatively distinguish the control from the hypomagnetic population as early as day 1 p.f. These observations are evident in panels **d**) through **f**) of Fig. 1. First, day 1 p.f. embryos in the hypomagnetic chamber exhibit greater eccentricity, suggesting accelerated development. **d**) depicts all day 1 images of batch B2 arranged by increasing eccentricity. By 24 hours p.f., most embryos in the hypomagnetic population have progressed beyond the circular-shaped egg stages, exhibiting a more elongated, bean-like shape. Day 1 images have frames color-coded based on the health assessment of the tadpoles by day 3 (see Supplementary Section SI7: Green indicates healthy tadpoles; orange indicates one health condition; red indicates multiple health conditions; and black indicates those that were deceased by day 1 p.f.). The images also show the major and minor axes of each embryo, as determined by the algorithm to calculate eccentricity described in Section 4. Second, hypomagnetic tadpoles appear paler in color in both day 2 and day 3 images. **e**) displays the three least and three most yellow healthy tadpoles for each condition from batch B2 by day 3, as identified by the algorithm detailed in Section 5. Third, hypomagnetic tadpoles tend to be longer and are typically at more advanced developmental stages compared to control tadpoles. **f**) highlights this point by depicting the five shortest and the five longest healthy tadpoles for each condition from batch B7 by day 3, after segmentation by the algorithm described in Section 6.

We then conducted the following gross morphological analysis, including positive control runs, to quantify the qualitative differences observed. Throughout our study, we aimed to minimize human intervention by ensuring that our image analysis is nearly fully automated (with a few exceptions detailed in Supplementary Section SI13). In addition, we propose that key morphological measures, derived from Nieuwkoop and Faber (NF) [15] stage-labeled images from reliable sources such as Xenbase [16], could be effectively used to characterize embryo developmental stages; we provide select examples to support this approach in the Supplementary Information (see Supplementary Figs. SI10, SI12, SI14, SI16, SI33, SI35, and SI37). We also aimed to provide multiple objective measures to corroborate each morphological observation. While the absolute magnitude of the effect depends on the measure chosen (for example, in the data of Section 4, a 20% increase in eccentricity corresponds roughly to a 1% decrease in solidity; both measures are good predictors of the same process of accelerated development, see Supplementary Figs. SI9 and SI15), we also consistently calculated a range of effect-size and effect-change metrics; these metrics are magnitude-insensitive because they standardize differences, being mostly reliable statistical indicators of the morphological distinctions between the control and hypomagnetic tadpole populations, independent of absolute scale. Our confidence in the presented results thus arises from a comprehensive analysis involving 19 distinct morphological measures, four effect-size metrics, and four effect-change metrics, applied across three days of imaging and tracking over 2,750 individual tadpoles.

a) hypomagnetic chamber:
AC+DC shielding

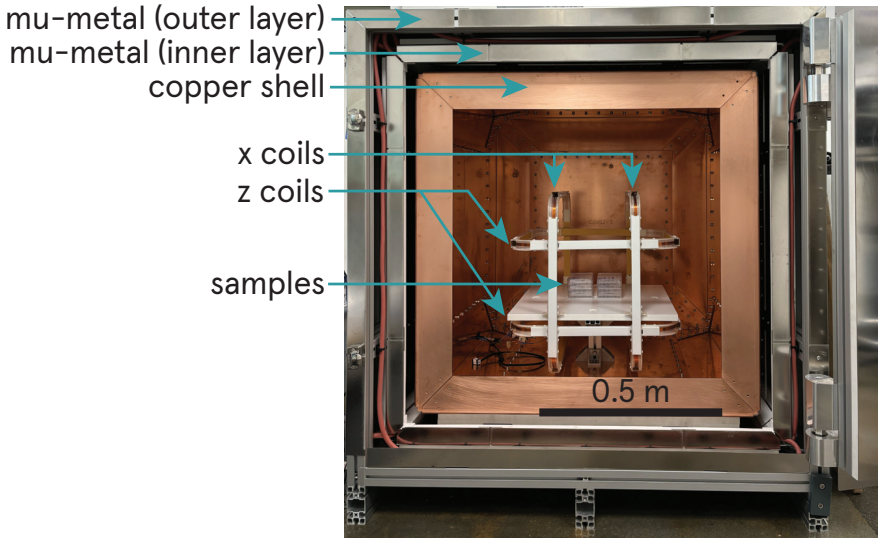

b) temperature calibration

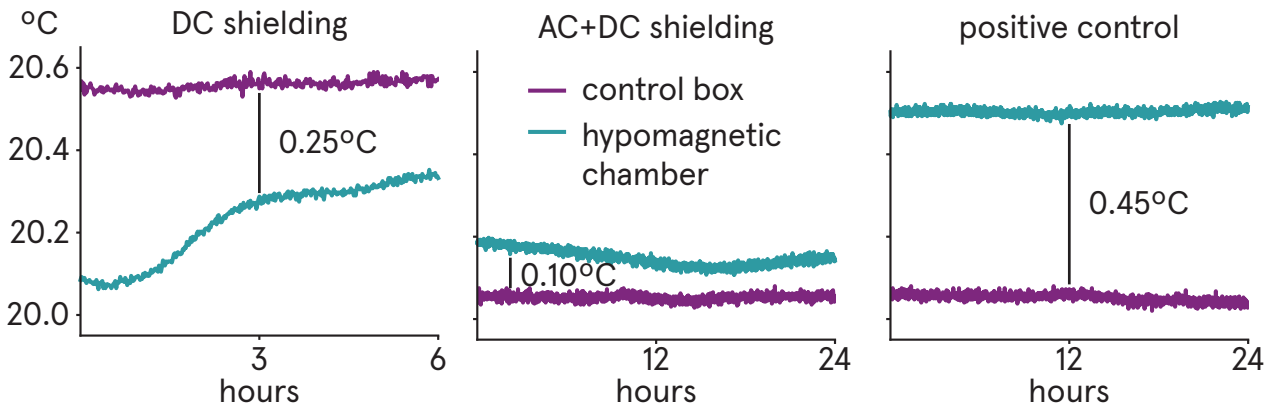

c) typical 3-day tadpole development

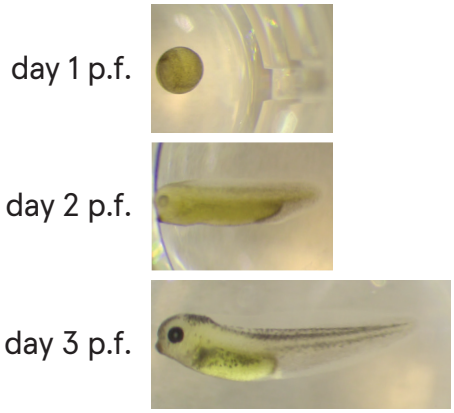

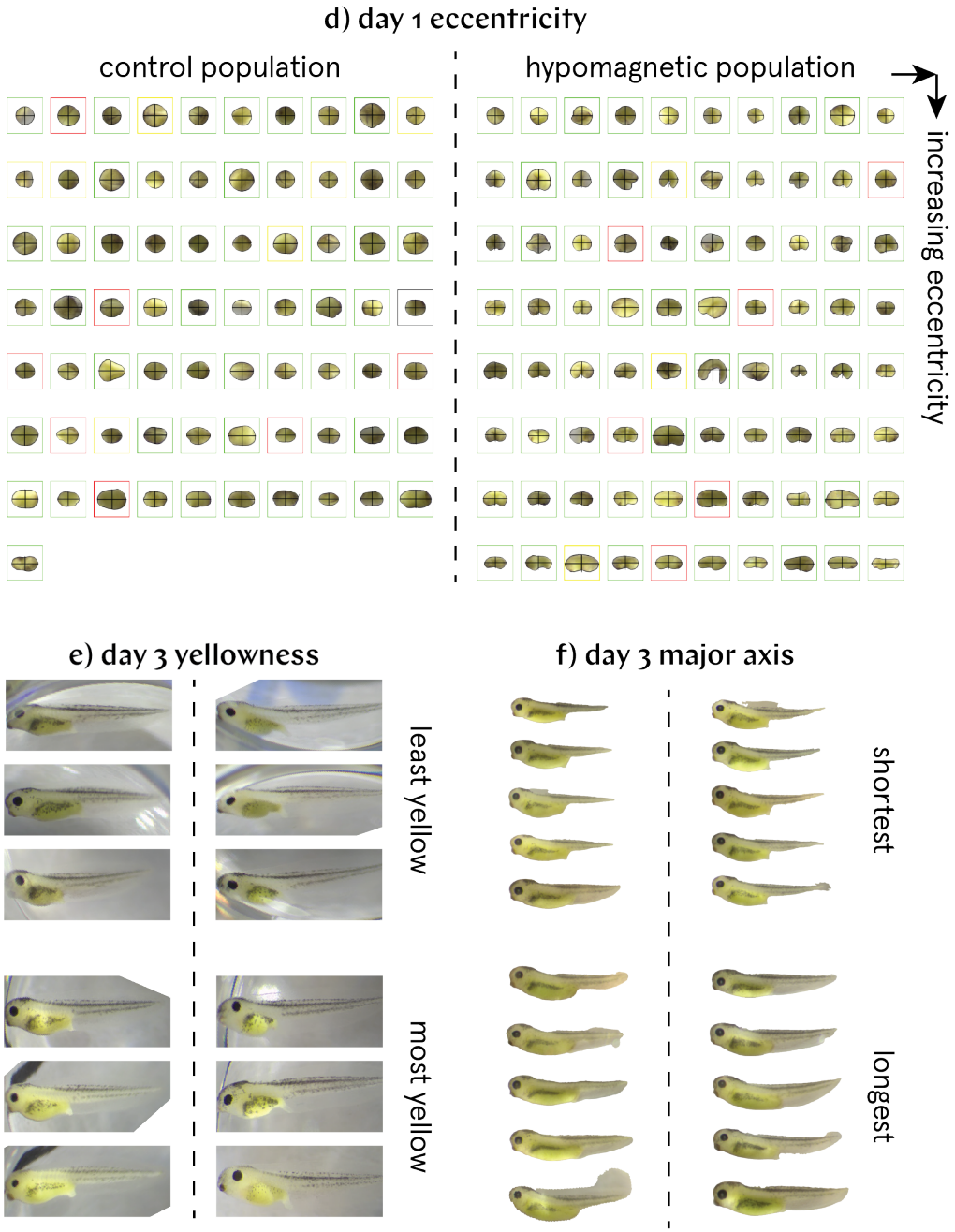

Fig. 1: Environmental conditions are well-controlled, and the differences between control and hypomagnetic populations are qualitatively evident. **a)** The hypomagnetic chamber is equipped with both AC (copper shell) and DC (mu-metal) shielding, and x and z coils for positive control runs; the sample placement is shown. **b)** Temperature calibration reveals nearly identical temperatures within the hypomagnetic chamber and the control box, with a maximum temperature difference of 0.45°C during positive control runs. **c)** Representative images depict the 3-day development of individually tracked tadpoles, totaling over 2,750 individuals. **d)** Day 1 images of batch B2, ordered by increasing eccentricity, show that the hypomagnetic population exhibits significantly higher eccentricity. **e)** Least and most yellow tadpoles of batch B2 on day 3; those from the hypomagnetic population exhibit noticeably less yellow pigmentation. **f)** Shortest and longest tadpoles of batch B7 on day 3; the hypomagnetic population tends to be longer, suggesting accelerated developmental progression.

4. The hypomagnetic field increases the eccentricity of day 1 embryos

At day 1 p.f., we observed frog embryos at various developmental stages, which we determined to range from NF stages 18 to 24 with the help of a standard table [15, 16]. During these stages, the embryos transition in shape from egg-like to bean-like and eventually to a more elongated, worm-like form.

To quantify our qualitative observation that frog embryos in hypomagnetic conditions exhibit accelerated development compared to control embryos already by this time point, we calculated morphological metrics assessing deviation from circularity—namely, eccentricity, elongation, roundness, and solidity. All four metrics consistently confirm our initial qualitative observation of advanced development under hypomagnetic conditions; they are detailed in Supplementary Section SI17, with a particular focus on eccentricity in the main text. Our code fits an ellipse to each day 1 p.f. image, defining the embryo's eccentricity as $e \equiv \sqrt{1 - \frac{b^2}{a^2}}$, where b and a are the minor and major axes of the fitted ellipse, respectively.

Results for the eccentricity of day 1 images are presented in Fig. 2. A detailed guide on how to read the analysis plots is available in Supplementary Section SI74. Due to significant batch-to-batch variability, we present the normalized plots in the main text, where each batch is scaled relative to the average control value. The non-normalized data are presented in the Supplementary Information. In the figure, batches B1–7 correspond to experimental runs, while batches +1–3 represent positive control runs, where a magnetic field simulating Earth's is applied within the hypomagnetic chamber (see Supplementary Section SI11). Throughout the plots, magnetic field conditions are denoted as C for control and H for hypomagnetic. The plots alternate between results for all tadpoles and for those classified as healthy based on the human scoring criterion described in Supplementary Section SI7.

In the **a**) and **b**) violin plots, each tadpole's value is represented by a horizontal line. The violin width reflects the kernel density estimation of the data distribution at that value. It is quantitatively evident that eccentricity is higher for tadpoles in hypomagnetic conditions, indicating a more elongated shape. In the non-normalized version of these plots, available in Supplementary Section SI19, we provide predicted tadpole stages based on elongation

from a few stage-labeled reference images found in Xenbase [16].

The eccentricity in tadpoles exposed to hypomagnetic conditions exceeds that of control tadpoles by nearly 20%. Plot **c**) illustrates the average eccentricity for both control and hypomagnetic conditions across batches, along with their 95% confidence intervals (as detailed in Supplementary Section SI16). The standard deviation of the mean plotted in **a**) and **b**) reflects the variability or dispersion in the data; in contrast, the 95% confidence interval in **c**) emphasizes the accuracy of the estimate, indicating the range within which the true population mean is likely to fall with 95% confidence. The aggregate values for all experimental runs (B1–7) and all positive control runs (+1–3) are also shown. For normalized plots, each data point is adjusted relative to its corresponding control within the batch, while for non-normalized plots, the raw data is used despite batch-to-batch variability. Data aggregation is performed prior to statistical analysis.

Our dataset is generally non-parametric, so we also examine the median as a robust measure of central tendency. In plot **d**), we apply bootstrapping (explained in Supplementary Section SI16) to estimate the median difference in eccentricity between the control and hypomagnetic groups. The median eccentricity for tadpoles exposed to hypomagnetic conditions exceeds that of the control group by also nearly 20%.

In plots **e**) and **f**), we evaluate several measures of effect size (details in Supplementary Section SI14). Notably, both Cohen's d and Cliff's Δ (shown in **e**)), which are commonly used in biostatistics [17], tend to produce large and potentially overestimated values in our dataset. In contrast, Binhi's E (shown in **f**)), a metric specifically designed for weak magnetic field effects in biology [1], more closely aligns with the net effects observed in plots **c**) and **d**); it estimates that the effect size of the hypomagnetic condition on eccentricity in day 1 embryos is again approximately 20%. Binhi's E quantifies the effect size by comparing the difference in the groups' means relative to their combined variability, accounting for both the magnitude and uncertainty of the measurements. We find that the visibility ν (also shown in **f**)) reliably yields a conservative estimate of effect size. Visibility ν is analogous to signal-to-noise, as it expresses the relative difference in the groups' means as a percentage

of their sum, providing a conservative estimate when the groups are close in magnitude. Below each plot, we also display the p value of a statistical test comparing the control and hypomagnetic populations (details in Supplementary Section SI74); points below the red dashed line indicate that the differences are statistically significant at the 0.01 level.

We provide a quantitative comparison of the observed accelerated development in terms of NF canonical stage numbers [15] in the Supplementary Information, using all day 1 measures of deviation from circularity—namely, eccentricity, elongation, roundness, and solidity (see Supplementary Figs. SI10, SI12, SI14, and SI16). These metrics were calculated from a few NF stage-labeled images sourced from Xenbase [16], offering an objective method to assess embryonic developmental stages.

The variability in major axis length for control embryos in day 1 p.f. images closely aligns with the 38% maximum difference reported in [14] for over 2,000 similar stage embryos. In contrast, the hypomagnetic embryos exhibit approximately 20% greater variability (see discussion in Supplementary Section SI63).

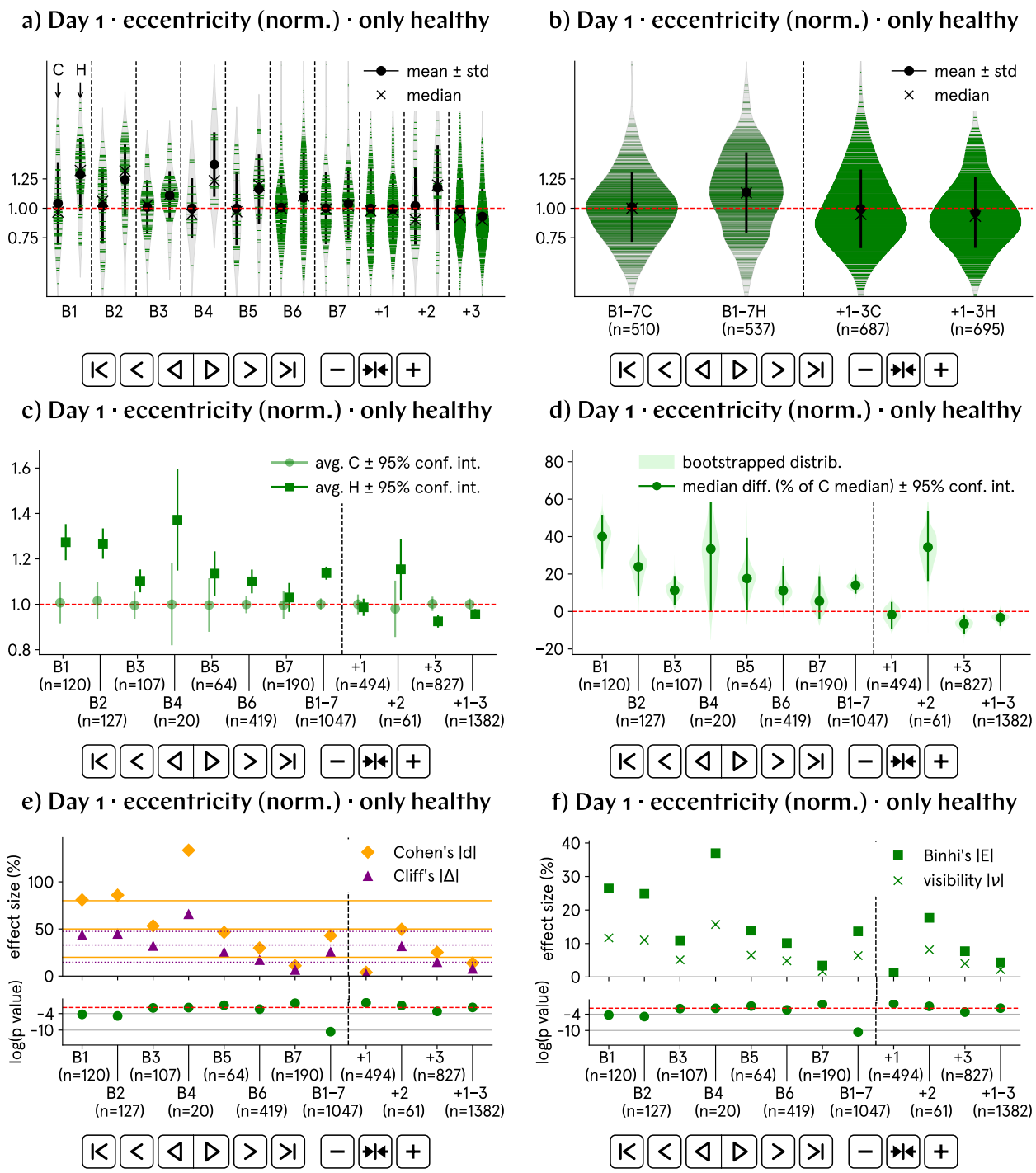

Fig. 2: At day 1 p.f., the eccentricity of hypomagnetic embryos is approximately 20% higher than that of the control population. **a)** and **b)** Normalized eccentricity by batch and aggregate data; B1–7 represent experimental runs, and +1–3 correspond to positive control runs, in which an artificial magnetic field inside the hypomagnetic chamber simulates Earth's. **c)** and **d)** Analysis of the population averages and medians further support the observed 20% increase in eccentricity. The abscissa points labeled B1–7 and +1–3 represent the aggregate values for the experimental and positive control runs, respectively. **e)** and **f)** Effect size metrics, namely Cohen's d and Cliff's Δ, and Binhi's E and the visibility ν, confirm a medium to large effect, consistently reflecting the 20% level difference.

5. The hypomagnetic field decreases the yellowness of day 2 tadpoles

We qualitatively observed a difference in the yellow coloration of tadpoles which were exposed to hypomagnetic conditions. The yellow coloration in tadpoles is due to the presence of carotenoid and pteridine pigments [18] (one study also cites flavin pigments [19]), which absorb light in the blue spectrum and reflect yellow and orange wavelengths, resulting in the tadpoles' characteristic yellow hue. After confirming that the ambient light environment was similar between the hypomagnetic and control groups (see Supplementary Fig. SI8 for light intensity and spectral comparison), we inquired whether the magnetic field itself could be directly related to these observed differences.

To quantify the color differences, we calculated several color metrics related to yellowness: L*a*b* yellowness, RGB yellowness, the Yellowness Index, and HSV yellowness. These metrics are described in detail in Supplementary Section SI26, with a primary focus on L*a*b* yellowness in the main text. All four metrics indicated distinct color development under hypomagnetic conditions. Although color differences are quantitatively evident in both day 2 and day 3 images, our analysis is exclusively for day 2 images. This is because day 3 images were taken after tadpole fixation with formalin, a process known to alter tissue color.

The L*a*b* color space [20] is designed for perceptual uniformity, meaning that small changes in objective color correspond to similar perceived differences. Unlike traditional color spaces such as RGB or CMYK, L*a*b* separates luminance from chromatic information, making it widely used in image processing for more accurate color representation. The b* channel, in particular, captures the blue-yellow axis, with positive values indicating increased yellowness. To simplify analysis, in Fig. 3 we present results for the b* channel—referred to as L*a*b* yellowness—in normalized plots, with each batch scaled relative to the average control value; the non-normalized data is presented in the Supplementary Information.

The violin plots **a**) and **b**) consistently show lower L*a*b* yellowness for tadpoles in hypomagnetic conditions. This effect, observed at the 5% level for day 2 images, is confirmed by both the average and bootstrapped median values plotted in **c**) and **d**), respectively, as well as by the magnitude of Binhi's E in **f**). Importantly, no color difference is seen in the

positive control tadpoles, which were raised inside the hypomagnetic box with an applied magnetic field mimicking Earth's. This result supports a mechanism through which the observed color change is driven primarily by the altered magnetic field conditions.

To investigate the cause of reduced yellow pigmentation, we examine the sources of pteridine and carotenoid in *Xenopus* embryos.

Tadpoles are capable of synthesizing pteridines as early as NF stages 39–40 [21], which occur well after the 2 day p.f. mark; therefore, synthesized pteridines could not account for the observed color changes already visible in day 2 p.f. images.

Carotenoids are either deposited in the egg during oogenesis or ingested from the diet after hatching. Since tadpoles do not begin feeding until well after day 3 p.f., all carotenoids present at this stage must originate from the yolk. Carotenoid content is reduced in amphibians that have undergone pituitary gland removal, leading to paler coloration [19]. In *Xenopus* tadpoles, the pituitary gland begins to form around NF stages 24–25 [15], *i.e.*, before our day 2 images are captured. However, the gland only starts to secrete hormones between stages NF 46–48 (5–6 days p.f.) [15], which is beyond the time frame of our study. Consequently, we do not believe the color differences we observe are of hormonal origin.

The visible changes in color during early development might thus reflect the metabolic use of the yolk's contents, including the pigments [22]. The specific concentrations of carotenoids and pteridines in *Xenopus* yolk are not well-documented and can vary depending on factors like maternal diet, environmental conditions, and species [21]. The major yolk protein, vitellogenin, is a lipoprotein that acts as a nutrient source for the developing embryo. While vitellogenin itself lacks color, it often binds to carotenoids, which contribute to the yellowish hue of the yolk [23]. As vitellogenin is processed into yolk proteins like lipovitellin and phosvitin during embryogenesis, and the yolk is gradually consumed, the yellow color fades due to the depletion of carotenoids. This process may explain the slightly decreased yellow hue we observe in hypomagnetic tadpoles, which exhibit morphological markers indicative of accelerated embryonic development.

We did not assess the levels of the more commonly studied eumelanin pigment [24, 25]. At day 2 p.f., eumelanin levels remained low. While the binarization procedure detailed in Supplementary Section **SI26** improved the accuracy of yellow pigment assessment, it was less reliable as a good discriminator of dark pigments like eumelanin.

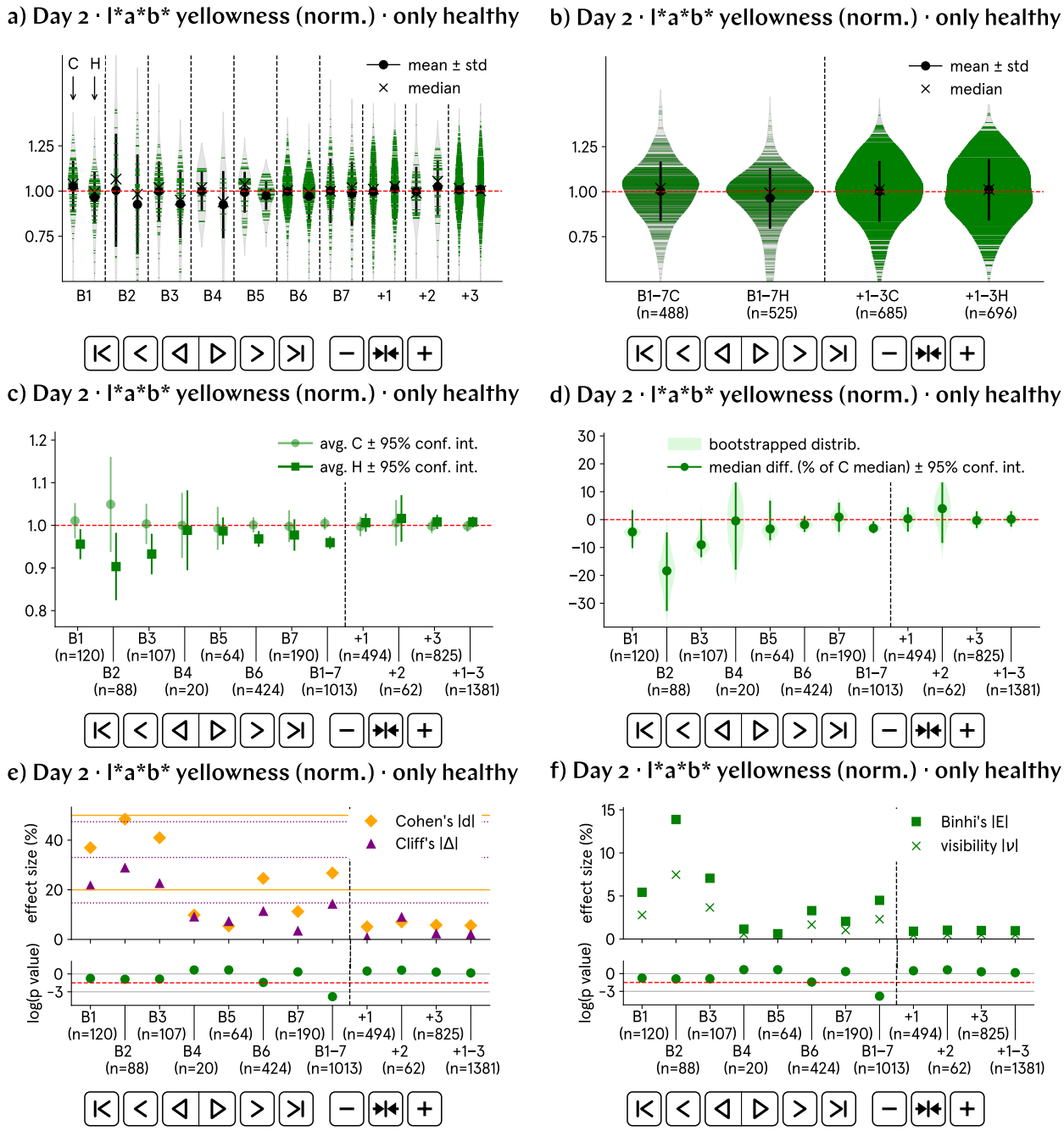

Fig. 3: At day 2 p.f., the L*a*b* yellowness of hypomagnetic embryos is approximately 5% lower than that of the control population. **a)** and **b)** Normalized L*a*b* yellowness by batch and aggregate data; B1–7 represent experimental runs, and +1–3 correspond to positive control runs, in which an artificial magnetic field inside the hypomagnetic chamber simulates Earth's. **c)** and **d)** Analysis of the population averages and medians further support the observed 5% decrease in L*a*b* yellowness. The abscissa points labeled B1–7 and +1–3 represent the aggregate values for the experimental and positive control runs, respectively. **e)** and **f)** Effect size metrics, namely Cohen's d and Cliff's Δ, and Binhi's E and the visibility ν, confirm a small to medium effect, consistently reflecting the 5% level difference.

6. The hypomagnetic field increases the length of day 3 tadpoles

The most striking evidence of accelerated development is the increased length of day 3 tadpoles exposed to hypomagnetic field conditions.

Day 3 tadpole images were segmented, and their major axes were calculated (as detailed in Supplementary Sections SI13 and SI35). The results are displayed in Fig. 4, with each batch normalized to the average control value. We opt not to present non-normalized data due to slight differences in magnification across batches.

Plots **a)** and **b)** illustrate the distribution of major axis lengths, with **b)** showing a distinct and quantitatively different violin shape for the hypomagnetic population.

The mean, shown in **c)**, and the bootstrapped median, in **d)**, both indicate an approximately 7.5% increase in major axis length for the hypomagnetic population. This result aligns with Binhi's E reported in **f)**. Additionally, both Cohen's d and Cliff's Δ, plotted in **e)**, classify this effect as medium in size. Notably, this effect is absent in the positive control tadpoles.

Additional morphological measures, namely perimeter, area, total curvature, solidity, elongation, and roundness (the latter reflecting the relationship between area and perimeter), as detailed in Supplementary Section SI35, consistently indicate more elongated and complex shapes in tadpoles exposed to the hypomagnetic conditions. These findings further reinforce the major axis results presented here.

We present a quantitative comparison of the observed accelerated development in terms of NF canonical stage numbers [15] in the Supplementary Information, using all day 3 measures that can be accurately reported in their non-normalized form (*i.e.*, without normalization by the control group average)—namely, solidity, elongation, and roundness (see Supplementary Figs. SI33, SI35, and SI37). Using NF stage-labeled images from Xenbase [16], we once more propose this as an objective approach for assessing embryonic development.

No evident difference in major axis is observed in day 2 images, as detailed in Supplementary Section S163. We hypothesize that this is due to the reduced robustness of segmentation in day 2 images, likely caused by the pale coloration of the tadpoles, which may affect the accuracy of the major axis analysis. Additionally, the imaging conditions on day 2 were less controlled, with live tadpoles that were not manipulated, potentially leading to distortions or tadpoles being out of the focal plane. In contrast, on day 3, the fixed tadpoles were carefully positioned with tweezers to lie flat and on their sides, yielding more reliable measurements.

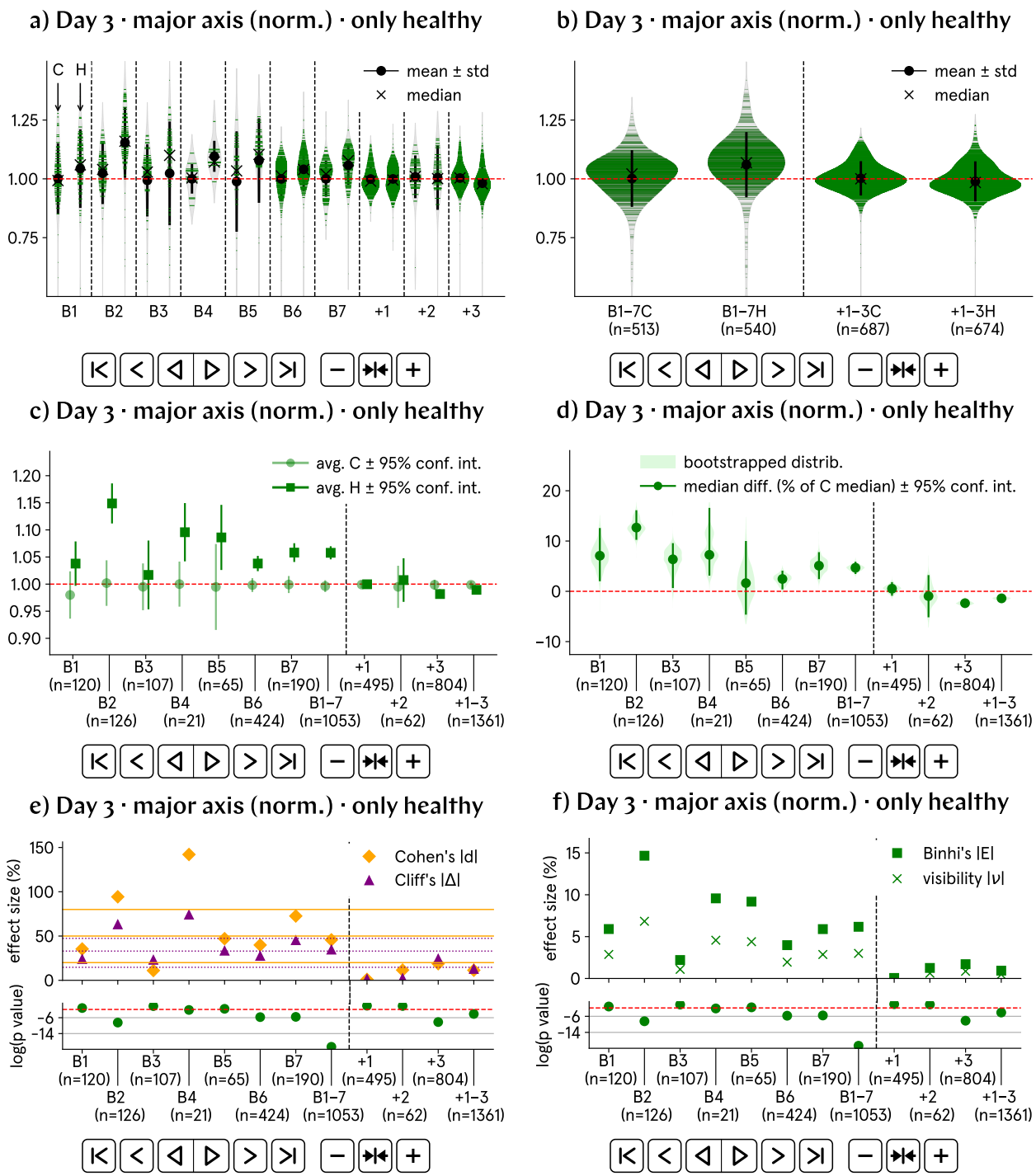

Fig. 4: **At day 3 p.f., the major axis of hypomagnetic embryos is approximately 7.5% higher than that of the control population.** a) and b) Normalized major axis by batch and aggregate data; B1–7 represent experimental runs, and +1–3 correspond to positive control runs, in which an artificial magnetic field inside the hypomagnetic chamber simulates Earth's. c) and d) Analysis of the population averages and medians further support the observed 7.5% increase in major axis. The abscissa points labeled B1–7 and +1–3 represent the aggregate values for the experimental and positive control runs, respectively. e) and f) Effect size metrics, namely Cohen's d and Cliff's Δ, and Binhi's E and the visibility ν, confirm a medium effect, consistently reflecting the 7.5% level difference.

7. The hypomagnetic field alters the morphological progression of tadpoles between days 2 and 3

In Fig. 5, we compare the day 2 to 3 progression of four key morphological properties of tadpole development, namely major axis length, curvature, convexity, and solidity. A Z-score metric for effect change normalizes the data by accounting for variability, allowing us to quantify changes in each property in relation to the mean values for both days (see Supplementary Section SI15). A positive Z-score difference indicates a greater deviation from the mean on day 3 compared to day 2. Although Z-score differences are our primary measure, additional metrics such as effect change visibility, percentage change, and relative difference were also calculated; they are described in detail in Supplementary Sections SI15 and SI46, and corroborate the trends observed in the Z-score analysis.

Plots **a**) and **b**) illustrate a predominantly positive Z-score difference for the major axis in the hypomagnetic group compared to the control. Plots **c**) and **d**) similarly reveal an overall positive Z-score difference for the total curvature, despite greater variability across batches. In contrast, convexity and solidity Z-score differences, depicted, respectively, in plots **e**) and **f**) and in plots **g**) and **h**), are lower for the hypomagnetic population. Across the four morphological properties analyzed, the Z-score difference metric reveals a divergence of approximately 0.5 units of standard deviation between the control and hypomagnetic populations, indicating a significant shift in the data associated with the hypomagnetic group.

The higher Z-score differences for major axis length and total curvature suggest accelerated morphological development under hypomagnetic conditions (as qualitatively observed in tadpole length and curvature differences between day 2 and 3 p.f. images in Fig. 1 **c**)). We interpret the average decrease in convexity and solidity Z-score differences as an indication of a faster increase in tadpole shape complexity. Lower convexity correlates with more indentations and protrusions, while lower solidity points to a more fragmented or irregular structure.

a) Day 2 to 3 · major axis (norm.) · only healthy Z-score diff.

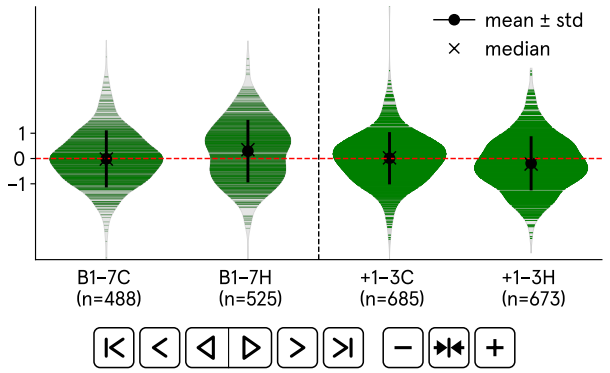

b) Day 2 to 3 · major axis (norm.) · only healthy Z-score diff.

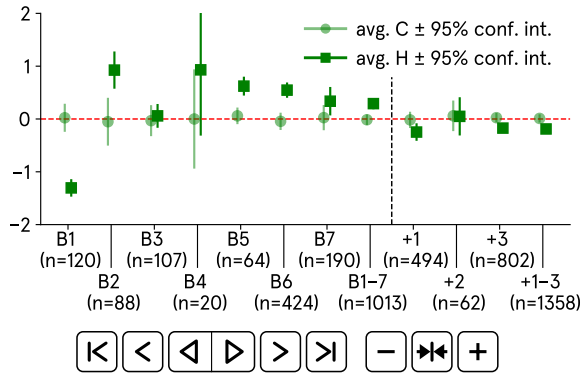

c) Day 2 to 3 · curvature (norm.) · only healthy Z-score diff.

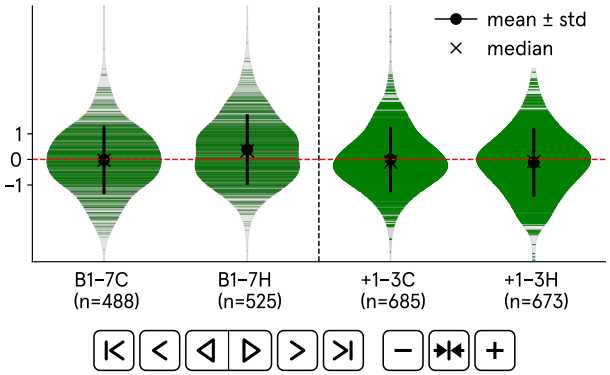

d) Day 2 to 3 · curvature (norm.) · only healthy Z-score diff.

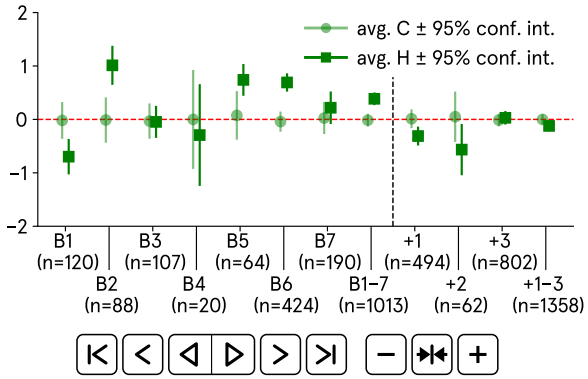

e) Day 2 to 3 · convexity (norm.) · only healthy Z-score diff.

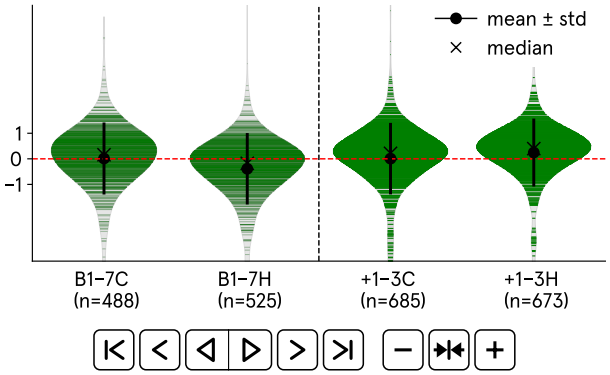

f) Day 2 to 3 · convexity (norm.) · only healthy Z-score diff.

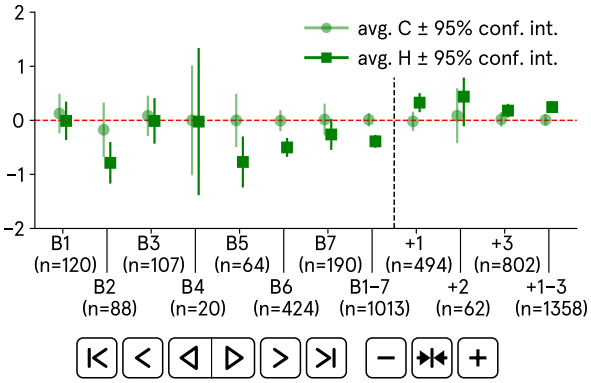

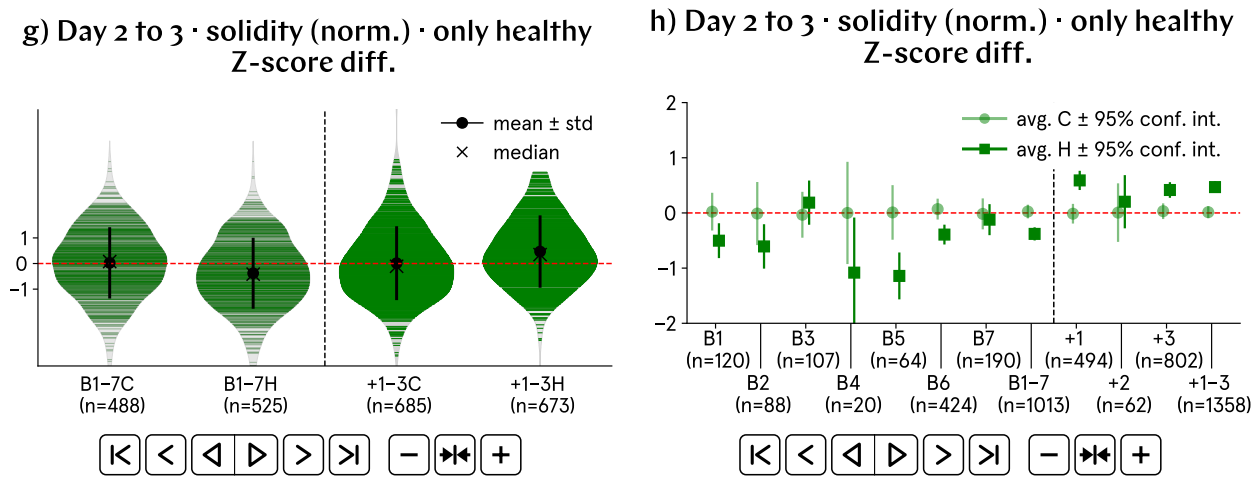

Fig. 5: **From day 2 to 3 p.f., the hypomagnetic conditions significantly influence the morphological progression of the tadpoles.** This progression is quantified, for each population (control or hypomagnetic), through differences in Z-scores at days 2 and 3 p.f. For the progression of the four morphological properties studied, the control and hypomagnetic populations differ by approximately 0.5 units of standard deviation, indicating a significant shift in the hypomagnetic population's data. The abscissa points labeled B1–7 and +1–3 represent the aggregate values for the experimental and positive control runs, respectively. **a)** and **b)** The major axis length in the hypomagnetic population exhibits a Z-score difference of approximately 0.5 higher than that of the control population. **c)** and **d)** A similar Z-score difference of about 0.5 higher for the total curvature is found in the hypomagnetic group. **e)** and **f)** In contrast, the convexity in the hypomagnetic population shows a Z-score difference around 0.5 lower than in the control group. **g)** and **h)** Solidity in the hypomagnetic population also has a Z-score difference nearly 0.5 lower than in the control. The higher Z-scores for major axis length and total curvature suggest accelerated morphological development under hypomagnetic conditions, while the lower Z-scores for convexity and solidity indicate a faster increase in shape complexity.

8. Discussion

After quantitatively analyzing over 8,000 images of nearly 3,000 viable tadpoles across 19 morphological measures, using four effect-size and four effect-change metrics, we conclude that magnetic fields as weak as the Earth's can have a macroscopic impact on biological processes such as embryo development.

We have demonstrated the existence of a link between Earth's minute DC magnetic field and basal tadpole physiology regulation that is present as early as one day p.f., for purposes likely *not* related to orientation, navigation, or homing. In the absence of the geomagnetic field, embryo development accelerates, a trend we observed and tracked over a three-day period in our experiments.

Potential influence of magnetic field variations. We cannot entirely dismiss the possibility that variations in magnetic field strength—*i.e.*, those occurring when plates are inserted or removed from the hypomagnetic chamber—may have influenced the baseline physiology of the tadpoles, rather than the constant hypomagnetic environment. This unlikely scenario would require a lasting biological response to short-term magnetic field variations.

Developmental response to the hypomagnetic field. It remains unclear whether *Xenopus* embryos sense Earth's magnetic field for a specific developmental purpose, or if their physiological response to hypomagnetic conditions simply reflects a deviation from an evolutionary adaptation that is arguably optimal for the geophysical environment in which the species evolved. Nonetheless, it is striking that in the absence of the geomagnetic field, the tadpoles consistently exhibit accelerated developmental speed, rather than a broad or indiscriminate alteration in developmental rhythms. This uniform response suggests the existence of a coordinated mechanism controlling the rate of development that includes magnetic cues. In rare instances, our data might be better modeled as a two-state system, which is consistent with responding and non-responding populations. These cases correspond to plots of type **b**) in which the aggregate violin suggests two distinct peaks in width, indicating a bimodal distribution.

Implications of accelerated embryogenesis. We speculate whether the observed accelerated development under hypomagnetic conditions could, in principle, increase

the incidence of embryo abnormalities and/or carcinogenesis. While no such effect has been detected in our data, it is possible that faster growth inherently raises the risk of developmental errors, as it has been previously reported in studies on the biological effects of hypomagnetic fields [1, 6, 26]. For example, hypomagnetic conditions have been linked to disturbances in the mitotic spindle [6], aligning with previous findings that weak magnetic fields alter cytoskeleton dynamics [1, 2, 7]. Consistent with our results, there are two literature reports that link the application of a weak magnetic field (rather than the elimination of a weak magnetic field)—specifically, 25 μT and 2 mT, albeit at low AC frequencies—with slowed development (rather than accelerated development) in *Xenopus* [27, 28].

Pigmentation changes and carotenoid depletion. There is one literature report linking the exposure to a weak magnetic field (of strength 0.5 mT) to an increase in eumelanin (dark) pigmentation in tadpoles [29]; while our study focused on yellow pigments, that result mirrors our own findings. We hypothesized that the depletion of yolk carotenoids could explain the paler-yellow appearance observed in hypomagnetic tadpoles. Carotenoids are known to be degraded by reactive oxygen species [30]. Overall levels of reactive oxygen species have been documented to increase under hypomagnetic field environments [31, 32]; an elevated reactive oxygen species concentration may thus have contributed to the observed reduction in carotenoid levels.

The effects of weak magnetic fields in biology have often been overlooked, including in studies of native organismal behavior, human health, and space exploration, as well as in guidelines for electromagnetic exposure. The rationale has been that the biological effects of weak magnetic fields are negligible because the field strengths are thought to be too small to trigger a biophysical sensing mechanism. Given the results of this study, however, this reasoning is flawed. Further investigation is therefore warranted, especially the use of omics and molecular techniques, to identify the nature of changes likely to be caused by the presence or absence of weak magnetic fields.

The fact that living beings can respond to magnetic field shifts of this magnitude thus usually comes as a surprise. To explain our findings, we note that organisms are traditionally thought to sense weak DC magnetic fields via three mechanisms (see Supplementary Section SI77).

In a small minority of cases, most notably in magnetotactic bacteria, cells contain biogenic magnetite crystals, which allow the organism to respond to magnetic fields like a classical compass [33]; these crystals must be large enough to overcome thermal motion and align with Earth's magnetic field [34, 35]. To date, there is only one report of ferrimagnetic material found in an amphibian, specifically in the newt [36]. Given that *Xenopus* is one of the most extensively studied biological model organisms worldwide, we find it unlikely, but not impossible, that such a magnetite-based magnetosensing mechanism is at play in this species, as cells containing large particles of magnetite would have likely been identified by now.

In another minority of instances, organisms possess specialized organs that function as conductive channels. When these channels intersect magnetic field lines, a voltage is induced according to the classical law of electromagnetic induction; such a voltage is then sensed by the organism. This is believed to explain how sharks and rays detect magnetic fields [37]. Given the structural complexity involved, we find it very unlikely that similar systems exist on day 1 p.f. *Xenopus* embryos, which contain fewer than 50,000 cells [38], yet are already capable of detecting the absence of Earth's magnetic field. In addition, the detection of DC magnetic fields through this mechanism requires the organism to move and cross magnetic field lines, and *Xenopus* embryos are not mobile until at least day 2 p.f.

In most cases, however, scientists have been unable to explain how weak magnetic fields impact biology, especially because the effects do not necessarily get larger when the magnetic field strength is increased, and are broadly nonspecific, occurring across diverse species and cell types [1, 2, 5, 8]. A chemical explanation that aligns with these observations exists but remains unverified microscopically and in living cells: electron spin-dependent chemical reactions [9, 39–41]. These reactions bear striking similarities to the simplest form of room-temperature technological quantum sensing in the solid-state [42, 43] and, at least *in vitro*, can detect magnetic fields using electron spin superpositions—even at room temperature [44]. In this hypothesis, organisms 'sense a magnetic field' by detecting changes in the physiological concentrations of reaction products, as the reaction rate responds to the magnetic field.

This hypothesis, which we favor, would itself be a surprise. If further experiments demonstrate that these or similar findings [45, 46] are a result of quantum sensing-like chemical reactions happening within living cells, the implications are major (see Supplementary Section SI78 for details). This will mean, first, that electron spin superpositions survive the strongly decohering environment of the cell for long enough to be used for function (*e.g.*, to sense and physiologically react to Earth's weak magnetic field); and second, that weak magnetic fields could, in principle, be quantum-engineered to influence the endogenous spin physics of biological matter, thereby enabling the up- and down-regulation of the machinery of the cell. While the effects reported so far remain largely nonspecific, enough knowledge of the spin physics within the specific proteins sustaining electron spin-dependent chemical reactions *in vivo* could, in principle, allow the targeted and predictable manipulation of physiological processes with weak magnetic fields.

9. Conclusion

We individually tracked the development of more than 2,750 *Xenopus laevis* embryos for three days under extremely carefully controlled magnetic field conditions. It is our assessment that other environmental factors such as temperature and light were controlled to a level where their variation would not be the origin of the observed biological effects. Through robust statistical analysis, we observed clear morphological changes in the tadpoles during experimental runs under hypomagnetic conditions of less than 1 nT; these largely disappear in the positive control runs.

We conclude that exposure to a hypomagnetic environment accelerates tadpole development in a measurable way. Therefore, *Xenopus laevis* embryos can detect and respond to the absence of Earth's minute DC magnetic field of approximately 50 μT as early as day 1 p.f.

Our data is publicly available and sufficiently robust to advance the scientific consensus that weak magnetic fields indeed exert measurable biological effects.

10. Author contribution

Following the CRediT taxonomy [47], each author confirms contribution of:

1) Alessandro Lodesani: conceptualization; methodology; investigation; data curation; validation; formal analysis; software; writing (original draft); writing (review and editing); and visualization;
2) Geoff Anders: conceptualization; methodology; writing (original draft); writing (review and editing); project administration; and funding acquisition;
3) Lykourgos Bougas: investigation; data curation; and formal analysis;
4) Tobias Lins: investigation; data curation; and formal analysis;
5) Dmitry Budker: conceptualization; supervision; and funding acquisition;
6) Peter Fierlinger: conceptualization; investigation; supervision; and funding acquisition;
7) Clarice D. Aiello: conceptualization; methodology; data curation; validation; formal analysis; software; writing (original draft); writing (review and editing); visualization; supervision; project administration; and funding acquisition.

11. Acknowledgements

We wholeheartedly thank: Michael Levin, from Tufts University, for suggesting the original idea of the experiment to P. F.; Arielle Gabalski for help with initial lab setup; Gabriel E. Bertolesi, from the University of Calgary, for first bringing to our attention the differences in developmental speed between the two tadpole groups; Vera D. Aiello, from the University of São Paulo, for first bringing to our attention the color differences between the two tadpole groups; Marko Horb and Nikko-Ideen Shaidani, from the National Xenopus Resource at the Marine Biological Laboratory, for early tadpole assessment and continuous frog husbandry support; Gabriel E. Bertolesi, from the University of Calgary, Paul Blank, from the NIH, Douglas Brash, from Yale University, Richard Fuisz, Maria Ingaramo and Andrew York, from Calico, Rod Kunz, Divya Shastry, and Alexandra Wrobel, from MIT-Lincoln Laboratory, Sergey Polyakov, from NIST, and Graham Timmins, from the University of New Mexico, for their valuable feedback on the manuscript; James Wiles, from the Wolfram Institute, for insights into image segmentation; and Jennilyn and Bret Gaitan, Oliver Carefull, and Melinda Bradley for project support.

We acknowledge the use of ChatGPT for improving the readability of the text and assisting with writing and debugging python code.

This experiment was partially funded by grants from the Faggin Foundation and Nevin Freeman.

Two authors (C. D. A. and G. A.) partially funded the conducted research. The remaining authors have no conflicts of interest to declare.

The Quantum Biology Institute is a California non-profit (501(c)(3) status pending) focused research organization [48] that performs basic research underpinning the quantum biology field in an open-science fashion. It is part of the Quantum Biology Ecosystem.

Bibliography

[1] V. N. Binhi and F. S. Prato, Biological effects of the hypomagnetic field: An analytical review of experiments and theories, PLoS ONE **12**, e0179340 (2017).

[2] Z.-H. Hadi and C. Simon, Magnetic field effects in biology from the perspective of the radical pair mechanism, J. R. Soc. Interface. **19**, 20220325 (2022).

[3] T. J. Zwang, E. C. M. Tse, D. Zhong, and J. K. Barton, A compass at weak magnetic fields using thymine dimer repair, ACS Cent. Sci. **4**, 329 (2018).

[4] R. J. Usselman, C. Chavarriaga, P. R. Castello, M. Procopio, T. Ritz, E. A. Dratz, D. J. Singel, and C. F. Martino, The quantum biology of reactive oxygen species partitioning impacts cellular bioenergetics, Sci. Rep. **6**, 38543 (2016).

[5] H. Wang and X. Zhang, Magnetic fields and reactive oxygen species, Int. J. Mol. Sci. **18**, 2175 (2017).

[6] W.-C. Mo, Y. Liu, H. M. Cooper, and R.-Q. He, Altered development of *Xenopus* embryos in a hypogeomagnetic field, Bioelectromagnetics **33**, 238 (2012).

[7] A. Bahrami, L. Y. Tanaka, R. C. Massucatto, F. R. M. Laurindo, and C. D. Aiello, Automated 1D Helmholtz coil design for cell biology: Weak magnetic fields alter cytoskeleton dynamics (2024), arXiv:2406.19555.

[8] F. Bertagna, R. Lewis, S. R. P. Silva, J. McFadden, and K. Jeevaratnam, Effects of electromagnetic fields on neuronal ion channels: A systematic review, Ann. N. Y. Acad. Sci. **1499**, 82 (2021).

[9] P. J. Hore and H. Mouritsen, The radical-pair mechanism of magnetoreception, Annu. Rev. Biophys. **45**, 299 (2016).

[10] L. Zastko, L. Makinistian, A. Tvarožná, *et al.*, Mapping of static magnetic fields near the surface of mobile phones, Sci. Rep. **11**, 19002 (2021).

[11] F. Hauksbee, An account of an experiment touching the production of light *in vacuo*, Philos. Trans. R. Soc. Lond. **26**, 149 (1709).

[12] L. Landler and G. Gollmann, Magnetic orientation of the common toad: Establishing an arena approach for adult anurans, Front. Zool. **8**, 6 (2011).

[13] M. K. Khokha, C. Chung, E. L. Bustamante, L. W. Gaw, K. A. Trott, J. Yeh, N. Lim, J. C. Lin, N. Taverner, E. Amaya, and N. Papalopulu, Techniques and probes for the study of *Xenopus tropicalis* development, Dev. Dyn. **225**, 499 (2002).

[14] A. Leibovich, T. Edri, S. L. Klein, S. A. Moody, and A. Fainsod, Natural size variation among embryos

leads to the corresponding scaling in gene expression, Dev. Biol. **462**, 165 (2020).

[15] P. D. Nieuwkoop and J. Faber, *Normal Table of Xenopus laevis (Daudin): A Systematical and Chronological Survey of the Development from the Fertilized Egg till the End of Metamorphosis*, 2nd ed. (Garland Pub., 1994).

[16] Xenbase, Xenbase Anatomy and Developmental Stages (2024), accessed: October 11, 2024.

[17] J. H. Zar, *Biostatistical Analysis*, 5th ed. (Pearson, Upper Saddle River, NJ, 2010).

[18] J. E. Mir, A. Nasrallah, N. Thézé, M. Cario, H. Fayyad-Kazan, P. Thiébaud, and H.-R. Rezvani, *Xenopus* as a model system for studying pigmentation and pigmentary disorders, Pigment Cell Melanoma Res. **00**, 1 (2024).

[19] J. T. Bagnara, M. E. Hadley, and J. H. Taylor, Regulation of bright-colored pigmentation of amphibians, Gen. Comp. Endocrinol. **2**, 425 (1969).

[20] M. D. Fairchild, *Color Appearance Models*, 3rd ed. (John Wiley & Sons, 2013).

[21] J. T. Bagnara and M. E. Hadley, *Chromatophores and Color Change: The Comparative Physiology of Animal Pigmentation* (Prentice Hall, Englewood Cliffs, NJ, 1973).

[22] P. Jorgensen, J. A. J. Steen, H. Steen, and M. W. Kirschner, The mechanism and pattern of yolk consumption provide insight into embryonic nutrition in *Xenopus*, Development **136**, 1539 (2009).

[23] J. D. Romano and T. R. Ziegler, Lipoproteins and carotenoids: Implications in embryogenesis and tissue differentiation, in *Carotenoids: Volume 4: Natural Functions*, edited by G. Britton, S. Liaaen-Jensen, and H. Pfander (Birkhäuser Verlag, 2002).

[24] G. E. Bertolesi, N. Debnath, H. R. Malik, L. L. H. Man, and S. McFarlane, Type II opsins in the eye, the pineal complex and the skin of *Xenopus laevis*: Using changes in skin pigmentation as a readout of visual and circadian activity, Front. Neuroanat. **15**, 784478 (2021).

[25] H. Liedtke, K. Lopez-Hervas, I. Galván, and et al., Background matching through fast and reversible melanin-based pigmentation plasticity in tadpoles comes with morphological and antioxidant changes, Sci. Rep. **13**, 12064 (2023).

[26] M. Asashima, K. Shimada, and C. J. Pfeiffer, Magnetic shielding induces early developmental abnormalities in the newt, *Cynops pyrrhogaster*, Bioelectromagnetics **12**, 215 (1991).

[27] S. Grimaldi, D. Pozzi, A. Lisi, S. Rieti, V. Manni, G. Ravagnan, L. Giuliani, T. Eremenko, and P. Volpe, Influence of the magnetic field on the tadpole metamorphosis, Int. J. Radiat. Med. **1**, 96 (2000).

[28] M. Severini, A. M. Dattilo, and A. D. Gaetano, Sublethal effect of a weak intermittent magnetic

field on the development of *Xenopus laevis* (daudin) tadpoles, Int. J. Biometeorol. **48**, 91 (2003).

[29] H. Z. Haghighi, G. Bertolesi, C. Simon, and S. McFarlane, Weak magnetic field effects on pigmentation in tadpoles, in *APS March Meeting* (American Physical Society, Minneapolis, 2024) Session BB02: Biological Physics at the Molecular Scale.

[30] G. Britton, S. Liaaen-Jensen, and H. Pfander, eds., *Carotenoids: Volume 4: Natural Functions* (Birkhäuser Verlag, 2008).

[31] R. Rishabh, H. Zadeh-Haghighi, D. Salahub, and C. Simon, Radical pairs may explain reactive oxygen species-mediated effects of hypomagnetic field on neurogenesis, PLoS Comput. Biol. **18**, e1010198 (2022).

[32] L. Tian, Y. Luo, A. Zhan, J. Ren, H. Qin, and Y. Pan, Hypomagnetic field induces the production of reactive oxygen species and cognitive deficits in mice hippocampus, Int. J. Mol. Sci. **23**, 3622 (2022).

[33] C. T. Lefevre and D. A. Bazylinski, Ecology, diversity, and evolution of magnetotactic bacteria, Microbiol. Mol. Biol. Rev. **77**, 497 (2013).

[34] J. Kirschvink and M. Walker, Particle size considerations for magnetite-based magnetoreceptors, in *Magnetite Biomineralization and Magnetoreception in Organisms: A New Biomagnetism*, Topics in Geobiology, Vol. 5, edited by J. Kirschvink, D. Jones, and B. McFadden (Plenum Press, New York, 1985).

[35] M. Meister, Physical limits to magnetogenetics, eLife **5**, e17210 (2016).

[36] J. Brassart, J. L. Kirschvink, J. B. Phillips, and S. C. Borland, Ferromagnetic material in the eastern red-spotted newt *Notophthalmus viridescens*, J. Exp. Biol. **202**, 3155– (1999).

[37] S. Johnsen and K. J. Lohmann, Magnetoreception in animals, Phys. Today **61**, 29 (2008).

[38] J. Cooke, Properties of the primary organization field in the embryo of *Xenopus laevis*. IV. Pattern formation and regulation following early inhibition of mitosis, J. Embryol. Exp. Morphol. **30**, 49 (1973).

[39] K. Schulten, C. E. Swenberg, and A. Weller, A biomagnetic sensory mechanism based on magnetic field modulated coherent electron spin motion, Z. Phys. Chem. **111**, 1 (1978).

[40] T. Ritz, S. Adem, and K. Schulten, A model for photoreceptor-based magnetoreception in birds, Biophys. J. **78**, 707 (2000).

[41] A. R. Jones, Magnetic field effects in proteins, Mol. Phys. **114**, 1691 (2016).

[42] J. R. Maze, P. L. Stanwix, J. S. Hodges, S. Hong, J. M. Taylor, P. Cappellaro, L. Jiang, M. V. G. Dutt, E. Togan, A. S. Zibrov, A. Yacoby, R. L. Walsworth, and M. D. Lukin, Nanoscale magnetic sensing with an individual electronic spin in diamond, Nature **455**, 644 (2008).

[43] J. M. Taylor, P. Cappellaro, L. Childress, L. Jiang, D. Budker, P. R. Hemmer, A. Yacoby, R. Walsworth, and M. D. Lukin, High-sensitivity diamond magnetometer with nanoscale resolution, Nat. Phys. **7**, 270 (2008).

[44] H. Lee, N. Yang, and A. E. Cohen, Mapping nanomagnetic fields using a radical pair reaction, Nano Lett. **11**, 5367 (2011).

[45] A. V. V. Huizen, J. M. Morton, L. J. Kinsey, D. G. V. Kannon, M. A. Saad, T. R. Birkholz, J. M. Czajka, J. Cyrus, F. S. Barnes, and W. S. Beane, Weak magnetic fields alter stem cell–mediated growth, Sci. Adv. **5**, eaau7201 (2019).

[46] N. Ikeya and J. R. Woodward, Cellular autofluorescence is magnetic field sensitive, Proc. Natl. Acad. Sci. U.S.A. **118**, e2018043118 (2021).

[47] Contributor role taxonomy (CRediT), `https://credit.niso.org/` (2024), accessed: October 11, 2024.

[48] A. Marblestone, A. Gamick, T. Kalil, C. Martin, M. Cvitkovic, and S. G. Rodriques, Unblock research bottlenecks with non-profit start-ups, Nature **601**, 188 (2022).

[49] S. Mcnamara, M. Wlizla, and M. E. Horb, Husbandry, general care, and transportation of *Xenopus laevis* and *Xenopus tropicalis*, Methods Mol. Biol. **1865**, 1 (2018).

[50] M. Wlizla, S. McNamara, and M. E. Horb, Generation and care of *Xenopus laevis* and *Xenopus tropicalis* embryos, Methods Mol. Biol. **1865**, 19 (2018).

[51] D. Budker, personal communication (2019).

[52] P. Fierlinger, personal communication (2019).

[53] A. E. Ruark and M. F. Peters, Helmholtz coils for producing uniform magnetic fields, J. Opt. Soc. Am. **13**, 205 (1926).

[54] C. Kindermann and J.-M. Hero, Pigment cell distribution in a rapid colour changing amphibian (*Litoria wilcoxii*), Zoomorphology **135**, 197 (2016).

[55] C. T. Rueden, J. Schindelin, M. C. Hiner, B. E. DeZonia, A. E. Walter, E. T. Arena, and K. W. Eliceiri, ImageJ2: ImageJ for the next generation of scientific image data, BMC Bioinformatics **18**, 529 (2017).

[56] J. Cohen, *Statistical Power Analysis for the Behavioral Sciences*, 2nd ed. (Lawrence Erlbaum Associates, Hillsdale, NJ, 1988).

[57] N. Cliff, Dominance statistics: Ordinal analyses to answer ordinal questions, Psychol. Bull. **114**, 494 (1993).

[58] J. Goedhart, Quantification of differences as an alternative to p values, Blog post on The Node (2018), accessed: October 11, 2024.

[59] The American Society for Testing and Materials, Test method for yellowness index of plastics, ASTM Standards **D1925-70** (1970).

[60] A. R. Smith, Color gamut transform pairs, SIGGRAPH Comput. Graph. **12**, 12 (1978).

[61] R. K. Adair, Constraints of thermal noise on the effects of weak 60-Hz magnetic fields acting on biological magnetite, Proc. Natl. Acad. Sci. U.S.A. **91**, 2925 (1994).

[62] D. J. Dunlop, Magnetite: Behavior near the single-domain threshold, Science **176**, 41 (1972).

[63] S. H. Eder, H. Cadiou, A. Muhamad, and M. Winklhofer, Magnetic characterization of isolated candidate vertebrate magnetoreceptor cells, Proc. Natl. Acad. Sci. U.S.A. **109**, 12022 (2012).

[64] B. L. Clites and J. T. Pierce, Identifying cellular and molecular mechanisms for magnetosensation, Annu. Rev. Neurosci. **40**, 231 (2017).

[65] J. L. Kirschvink and J. L. Gould, Biogenic magnetite as a basis for magnetic field detection in animals, Biosystems **13**, 181 (1981).

[66] S. E. Greene and A. Komeili, Biogenesis and subcellular organization of the magnetosome organelles of magnetotactic bacteria, Curr. Opin. Cell Biol. **24**, 490 (2012).

[67] O. Gorobets, S. Gorobets, and M. Koralewski, Physiological origin of biogenic magnetic nanoparticles in health and disease: From bacteria to humans, Int. J. Nanomedicine **12**, 4371 (2017).

[68] N. B. Edelman, T. Fritz, S. Nimpf, and D. A. Keays, No evidence for intracellular magnetite in putative vertebrate magnetoreceptors identified by magnetic screening, Proc. Natl. Acad. Sci. U.S.A. **112**, 262 (2015).

[69] G. Fleissner, B. Stahl, and P. Thalau, A novel concept of Fe-mineral-based magnetoreception: Histological and physicochemical data from the upper beak of homing pigeons, Naturwissenschaften **94**, 631 (2007).

[70] G. Falkenberg, K. Schuchardt, M. Kuehbacher, P. Thalau, H. Mouritsen, D. Heyers,

G. Wellenreuther, and G. Fleissner, Avian magnetoreception: Elaborate iron mineral containing dendrites in the upper beak seem to be a common feature of birds, PLoS ONE **5**, e9231 (2010).

[71] M. Walker, C. Diebel, and C. Haugh, Structure and function of the vertebrate magnetic sense, Nature **390**, 371– (1997).

[72] E. M. Pantelouris, B. Knox, and H. Wallace, Iron in amphibian oocytes and embryos, Exp. Cell Res. **32**, 469 (1963).

[73] T. Nomizu, K. H. Falchuk, B. L. Vallee, and B. L. Vallee, Zinc, iron, and copper contents of *Xenopus laevis* oocytes and embryos, Mol. Reprod. Dev. **36**, 419 (1993).

[74] J. L. Kirschvink, J. Brassart, and M. H. Nesson, Magnetite-based biological effects in animals: Biophysical, contamination, and sensory aspects. EPRI, Palo Alto, CA. Report TR–111901 (1998).

[75] U. E. Steiner and T. Ulrich, Magnetic field effects in chemical kinetics and related phenomena, Chem. Rev. **89**, 51 (1989).

[76] Z. Zeng, J. Wei, Y. Liu, W. Zhang, and T. Mabe, Magnetoreception of photoactivated cryptochrome 1 in electrochemistry and electron transfer, ACS Omega **3**, 4752 (2018).

[77] A. Ehrenberg, P. Hemmerich, F. Müller, and W. Pfleiderer, Electron spin resonance of pteridine radicals and the structure of hydropteridines, Eur. J. Biochem. **16**, 584 (1970).

[78] F. Müller, ed., *Chemistry and Biochemistry of Flavoenzymes* (CRC Press, 1991).

[79] M. J. Leask, A physico-chemical mechanism for magnetic field detection by migratory birds and homing pigeons, Nature **267**, 144 (1977).

[80] W. W. Cochran, H. Mouritsen, and M. Wikelski, Migrating songbirds recalibrate their magnetic compass daily from twilight cues, Science **304**, 405 (2004).

[81] H. G. Hiscock, T. W. Hiscock, D. R. Kattnig, T. Scrivener, A. M. Lewis, D. E. Manolopoulos, and P. J. Hore, Navigating at night: Fundamental limits on the sensitivity of radical pair magnetoreception under dim light, Q. Rev. Biophys. **52**, e9, 1 (2019).

[82] M. Cifra and P. Pospisil, Ultra-weak photon emission from biological samples: Definition, mechanisms, properties, detection and applications, J. Photochem. Photobiol. B **139**, 2 (2014).

[83] R. van Wijk and C. G. J. van Wijk, *Ultra-Weak Photon Emission: Characteristics, Origin, and Application* (Springer, 2024).

[84] N. F. Ramsey, A molecular beam resonance method with separated oscillating fields, Phys. Rev. **78**, 695 (1950).

[85] C. D. Aiello, M. Hirose, and P. Cappellaro, Composite-pulse magnetometry with a solid-state quantum sensor, Nat. Commun. **4**, 1419 (2013).

[86] E. D. Yorke, A possible magnetic transducer in birds, J. Theor. Biol. **77**, 101 (1979).

[87] J. Ashmore, Cochlear outer hair cell motility, Physiol. Rev. **88**, 173 (2008).

[88] J. R. Woodward, T. J. Foster, A. R. Jones, A. T. Salaoru, and N. S. Scrutton, Time-resolved studies of radical pairs, Biochem. Soc. Trans. **37**, 358 (2009).